Biochimica et Biophysica Acta 1858 (2017) 103–108

Contents lists available at ScienceDirect

Biochimica et Biophysica Acta

journal homepage: www.elsevier.com/locate/bbabio

Redox induced protonation of heme propionates in cytochrome *c* oxidase: Insights from surface enhanced resonance Raman spectroscopy and QM/MM calculations

Murat Sezer [a], Anna-Lena Woelke [b], Ernst Walter Knapp [b], Ramona Schlesinger [c], Maria Andrea Mroginski [a,*], Inez M. Weidinger [a,*]

[a] Institut für Chemie PC 14, Technische Universität Berlin, Strasse des 17. Juni 135, 10623 Berlin, Germany
[b] Institut für Chemie und Biochemie, Freie Universität Berlin, Fabeckstraße 36a, 14195 Berlin, Germany
[c] Institut für Experimentalphysik, Freie Universität Berlin, Arnimallee 14, 14195 Berlin, Germany

ARTICLE INFO

Article history:
Received 22 July 2016
Received in revised form 18 October 2016
Accepted 28 October 2016
Available online 31 October 2016

Keywords:
Cytochrome c oxidase
Proton pumping
Proton loading site
Surface enhanced Raman spectroscopy
QM/MM calculations

ABSTRACT

Understanding the coupling between heme reduction and proton translocation in cytochrome *c* oxidase (CcO) is still an open problem. The propionic acids of heme a_3 have been proposed to act as a proton loading site (PLS) in the proton pumping pathway, yet this proposal could not be verified by experimental data so far. We have set up an experiment where the redox states of the two hemes in CcO can be controlled via external electrical potential. Surface enhanced resonance Raman (SERR) spectroscopy was applied to simultaneously monitor the redox state of the hemes and the protonation state of the heme propionates. Simulated spectra based on QM/MM calculations were used to assign the resonant enhanced CH_2 twisting modes of the propionates to the protonation state of the individual heme *a* and heme a_3 propionates respectively. The comparison between calculated and measured H_2O—D_2O difference spectra allowed a sound band assignment. In the fully reduced enzyme at least three of the four heme propionates were found to be protonated whereas in the presence of a reduced heme *a* and an oxidized heme a_3 only protonation of one heme a_3 propionates was observed. Our data supports the postulated scenario where the heme a_3 propionates are involved in the proton pathway.

1. Introduction

Cytochrome *c* oxidase (CcO) is the terminal enzyme of the respiratory chain that pumps protons from the N to the P side of the membrane. The energy needed for this pumping process is gained from the catalytic reduction of oxygen to water, which takes place in the catalytic heme a_3-Cu_B binuclear center (BNC). The reaction sequence of catalytic oxygen splitting and transformation inside the BNC has been widely studied in the past [1–4] and is generally accepted these days. Not yet understood is, however, the coupling between the oxygen reaction and the proton pumping process. Oxygen reduction to water requires four electrons and protons that are delivered to the BNC via clearly defined pathways. Electrons are supplied one by one from the external redox protein cytochrome c making this process the rate limiting step of the whole cycle. Inside CcO the electrons have to pass a Cu_A and a heme *a* cofactor before they reach the BNC. In bacterial CcO the protons are supplied via two proton (K and D) channels that start at the protein entrance on the N side and end in close vicinity of the heme *a*-heme a_3 cofactors. Uptake of each electron is accompanied by uptake of two protons, one being used as chemical proton for oxygen reduction and one that ends up as a pumped proton. Orchestration of these events requires a tight interaction of the heme cofactors and their direct amino acid environment. Even more importantly a very defined sequence of electron transfer, proton transfer and oxygen reduction steps has to be present in order to guarantee that pumped protons do not move backwards or end up as chemical protons [5]. This precise sequence of events requires an advanced gating mechanism, which its exact nature is still discussed in the literature. Promising mechanistic scenarios for the protonation dynamics in CcO have been proposed based on calculations [6–10], their experimental verification is, however, often based on indirect measurements such as the kinetic isotope effect on the catalytic oxygen reaction [11].

To achieve the required unidirectionality of the proton translocation, the pumped protons have to be stored in a proton loading site (PLS) before arrival of the next electron further advances the pumping process. The PLS has therefore to be close to the BNC such that the stored proton can "feel" the presence of a new electron. A prominent candidate for the PLS in bacterial CcO is the heme a_3 propionate PrDa_3, as was suggested based on free energy computations [6]. However, under resting conditions this propionate forms a salt bridge to a nearby Arg481, rendering

* Corresponding authors.

http://dx.doi.org/10.1016/j.bbabio.2016.10.009
0005-2728/

its protonation highly unlikely. Theoretical calculations on C*c*O from *Bos taurus* have nevertheless shown that reduction of heme *a* is able to disrupt the strong bond between PrDa_3 and the nearby arginine, which makes PrDa_3 at least transiently accessible for protons [8].

The reaction sequence that includes PrDa_3 as PLS would start with reduction of heme *a* followed by proton transfer from Glu286 to PrDa_3. This change in protonation triggers electron transfer from heme *a* to heme a_3 and a second proton transfer from Glu286 into the catalytic binuclear heme a_3-Cu_B center. Proton 1 leaves the cofactor environment as a pumped proton possibly via the PrAa_3 propionate while proton 2 is used as a chemical proton in the oxygen reduction process. Although this scenario is widely accepted nowadays, a lot of questions remain: specifically the proton pumping pathway via the heme a_3 propionates is still under debate as direct evidence from experiments is still missing.

Vibrational spectroscopy is very suitable to probe protonation states of acid groups and thus is the technique of choice to study the above discussed reaction sequences in C*c*O. Specifically IR spectroscopy is very sensitive to the CO stretching vibration of carboxylic acids; it can however not exclusively probe the heme environment. IR difference spectroscopy was nevertheless performed by Behr et al. [12,13] to probe heme propionate protonation using a mutant with ^{13}C labelled propionates. The results indicated a protonated PrD*a* in the fully reduced enzyme.

In contrast to IR, resonance Raman (RR) spectroscopy probes specifically the heme cofactors and has been widely used in the past to analyze the structure of the two hemes in its resting state [14] and under turnover conditions [3,15,16]. Unfortunately, Raman spectroscopy is not sensitive to the polar CO vibration of the heme propionic acids. However, recently the corresponding vibrational modes of the protonation dependent CH_2 bending modes have been detected by H_2O minus D_20 RR difference spectroscopy [17,18]. Contrary to the IR data of Behr et al. these experiments showed protonation of all four heme propionates in the fully reduced enzyme.

We have recently shown that individual reduction of the two hemes in C*c*O can be controlled from the outside, when the enzyme is attached to an electrode that introduces electrons in a well defined manner [19]. Here, the electrode was functionalized in a way that the natural electron transfer pathway from Cu_A → heme a → heme a_3-Cu_B could be established. In contrast to other methods, which use photosensitive electron donors, electrons are continuously delivered and electron supply can be adjusted in a way that it matches its transfer rate in C*c*O under physiological conditions. Attachment to noble metal electrodes also has the advantage that one can apply surface enhanced resonance Raman (SERR) spectroscopy, which allows the use of much less protein. This technique has been used in the past for immobilized C*c*O [19,20] and other heme proteins [21–24]. Here, we will apply H_2O—D_2O SERR difference spectroscopy to monitor the redox dependent protonation state of the heme propionates. The results are compared to vibrational spectra derived from QM/MM calculations.

2. Material and methods

The *R. sphaeroides* strain JS100, containing the genetic information of subunit I of the *aa*$_3$-type C*c*O with a C-terminal 6xHis tag, was cultivated under aerobic conditions [25] and the enzyme was purified as previously described [19,26].

Electrochemically roughened Ag electrodes were incubated in an ethanolic solution of 3 mM 8-aminothiophenol (C8-NH_2) and 1 mM 6-mercaptohexanol (C6-OH). For electrostatic immobilization of C*c*O the coated electrodes were incubated in a solution containing 0.2 μM C*c*O, 20 mM Na-PBS (pH 8.0) and 0.1% (w/w) β-DM. For the D_2O experiments, the same buffer was prepared in D_2O and the pH with DCl adjusted. The pH/pD-shift was taken into account. The C*c*O coated Ag electrode was inserted as a working electrode into a homemade electrochemical cell [27]. An Ag/AgCl reference and a PT counter electrode were used in the measurements.

SERRS measurements were performed with the 442 nm line of a HeCd laser (VM-TIM, HCL-100). Spectra were recorded using a confocal Raman spectrometer (LabRam HR-800, Jobin Yvon). The laser power on the sample was 150 μW. Accumulation time was 60 s (30 cycles) for each spectrum. The electrode was constantly rotated to avoid photoreduction.

The hybrid QM/MM calculations were performed using the crystal structure of *R. sphaeroides* (PDB entry: 1M56) as starting geometry. The C*c*O was embedded in a lipid bilayer consisting of POPC lipid molecules. In this structural model, the enzyme is in its fully reduced state with Fe(II) for heme a_3 and heme *a*, and reduced Cu_B. Furthermore, the Fe of heme a_3 has a hydroxyl group as axial ligand. In addition, the Y288 is deprotonated, D407 is protonated and the D286 is protonated in agreement with Goyal and Cui QM/MM model [7]. QM/MM geometry optimization of heme *a* and heme a_3 with the corresponding protein environment was performed considering different protonation states of their PrA and PrD propionic acids. For this purpose, two separate QM-regions were defined: one containing the heme *a* (without the farnesylethyl tail) and the two ligating histidines (His102 and His421); and a second QM region including heme a_3 (without the farnesylethyl tail), the ligating His419 and the hydroxyl group bounded to the iron. The QM fragments were described with DFT at the B3LYP/6-31G* level of theory, whereas the MM part was treated with the empirical CHARMM22 force field [28]. The coupling between the QM and MM regions was described through the electrostatic embedding model using the charge-shift scheme [29]. Geometry optimizations were performed with the modular program package ChemShell [30] using the limited memory quasi Newton L-BFGS algorithm working with delocalized internal coordinates. The optimized structures of the four structural models were taken as input for the computation of the Raman spectra, which were performed for the unlabeled and the corresponding propionic-acid-deuterium-labeled species. These calculations were done following the procedure described in detail in Ref. [31].

3. Results

C*c*O from *R. sphaeroides* was grown, purified and immobilized on electrodes as described previously [19]. Electrochemically roughened Ag electrodes were firstly functionalized with a 1:3 mixed C8-NH_2/C6-OH terminated self assembled monolayer and subsequently put into a solution containing 0.2 μM C*c*O for 4 h to allow for electrostatic binding of the protein. The electrodes were then washed and inserted as a working electrode into a special designed spectro-electrochemical cell [27,32]. This immobilization procedure has proven to establish a good electrical communication between the electrode and the heme cofactors with an intact catalytic binuclear center (BNC).

SERR spectroscopic measurements were performed using the 442 nm excitation line of a HeCd laser, which is in resonance with the reduced species of C*c*O. The electrochemical cell was purged with Argon leaving only a very small amount of oxygen in the probe volume. We will in the following correspond to this situation as the one in presence of low concentrated oxygen. The working electrode was left at open potential and sodium dithionite in excess concentration was added as a chemical reductant. Under this condition, the SERR spectrum shown as trace A in Fig. 2 was recorded. The same experiment was repeated in the absence of dithionite but with the working electrode set to an applied potential of −250 mV vs. Ag/AgCl, which corresponds to an overpotential of −450 mV with respect to the redox potential of heme *a*. The so recorded SERR spectrum is shown as trace B in Fig. 2. Both spectra (A and B) show similar features that correspond to the typical porphyrin ring vibrations of a reduced heme species but with different intensities. Specifically the position of the most prominent porphyrin ring vibration ν_4 at 1356 cm^{-1} demonstrates that the enzyme is in both cases at least partially reduced. Furthermore the bands

at 1518 cm^{-1} and 1585 cm^{-1}, which can be clearly seen in both spectra, have been assigned to the reduced heme *a* of C*c*O before [33]. A specific marker band for the reduced heme a_3 is at 1663 cm^{-1} that corresponds to the heme a_3 formyl stretching vibration. This band is only visible in spectrum A but is missing in B. We thus conclude that in spectrum A both hemes are reduced while in spectrum B heme a_3 remains still oxidized. Using 442 nm excitation we cannot distinguish whether heme a_3 in spectrum B is in its Fe(III) state or in its intermediate oxoferryl state. However, previous spectro-electrochemical investigations of C*c*O on electrodes, where oxygen could not be completely eliminated [19,34], show a similar behaviour and here the Fe(III) state was identified.

We explain the different behavior when using either a chemical or an electrochemical reductant with the different kinetics of the electron supply. In both cases (A and B) low amounts of oxygen are present that are transformed to water at the heme a_3-Cu_B site leaving heme a_3 subsequently in its oxidized state. Electron supply from the electrode is slower that the rate of oxygen binding thus we observe heme a_3 predominantly in its oxidized Fe(III) state. Electron supply from a chemical reductant is on the other hand much faster leading to a situation where oxygen binding becomes rate limiting. In this case we observe a fully reduced enzyme.

To eliminate the influence of oxygen, the experiments were repeated in an anaerobic box, which has been described by us in detail before [19]. Reduction of C*c*O was initiated by applying a negative overpotential at the working electrode. A SERR spectrum recorded under completely oxygen free conditions at an applied potential of −400 mV vs. Ag/AgCl is shown in trace C of Fig. 2. Here again the band at 1663 cm^{-1} becomes clearly visible together with a high intensity of the reduced ν_4 band at 1356 cm^{-1} indicating that we have a fully reduced enzyme present.

In a next step we aimed to monitor the corresponding protonation state of the heme propionates. We recorded SERR spectra of immobilized C*c*O in H_2O and D_2O buffer solution (Fig. S1). Similar to the experiments mentioned before, C*c*O was either reduced chemically by addition of dithionite or electrochemically by an external electrode potential. The latter experiments were conducted again inside and outside the anaerobic box. The resulting SERR H_2O—D_2O difference spectra are presented in Fig. 3. Using dithionite as chemical reductant (trace A in Fig. 3) negative bands at 1179 cm^{-1}, 1218 cm^{-1}, 1232 cm^{-1}, 1250 cm^{-1} and 1310 cm^{-1} are visible similar to the ones obtained by Egawa et al. [17]. Furthermore we observed two more negative bands appear at 1149 cm^{-1} and 1283 cm^{-1} and most likely a negative band at 1330 cm^{-1}. The latter is not shown in Fig. 3 as in this region the strongly enhanced ν_4 vibration of the porphyrin ring is appearing resulting in a strong error of the H/D difference spectra. In the electrochemically reduced enzyme and in the presence of low concentrated oxygen (trace B in Fig. 3) all negative bands, except the band at 1250 cm^{-1}, disappear. In the absence of oxygen the same negative bands, as observed by chemical reduction, could be seen again in the H_2O—D_2O difference spectrum (trace C in Fig. 3) albeit with different relative intensities. The most prominent differences between trace A and C belong to the relative decrease of the bands at 1232 cm^{-1} and 1250 cm^{-1} and the shift of the bands between 1310 cm^{-1} and 1304 cm^{-1}.

To assign the difference bands observed in the SERR spectra, hybrid QM/MM calculations of Raman spectra were performed for the heme *a* and heme a_3 cofactors. Analysis of the Raman spectra was restricted to the 1050–1350 cm^{-1} window where H/D isotopic shifts of PrA and PrD are expected. The results are shown in Fig. 4 and Table S1. For the sake of clarity, we restricted the displayed data to the vibrations, which show significant H/D isotopic shift or a strong increase in Raman activity upon deuteration. The results presented in Fig. 4 were done considering only one protonated side chain at a time since double protonation would imply large perturbation of the heme pockets, and thus is not very likely to occur. Test calculations with simultaneous protonation of PrA*a* and PrD*a* showed that the corresponding difference spectrum is a superposition of the respective spectra with either a deuterated PrA, or a deuterated PrD (Table S2). Thus, double protonation cannot be completely excluded from our experimental data.

Following this filtering procedure, almost all experimental bands observed in the interval 1100–1350 cm^{-1} could be straightforwardly assigned to CH_2-deformation modes located at the propionic acids of the hemes. The only exception is the peak at 1250 cm^{-1}. Very close to this position, we predict CH_2 deformation modes due to PrA*a* and from both acids of heme a_3. Thus, for this band an unambiguous assignment is not possible solely by comparison of calculated and experimentally observed band positions. The final vibrational assignment of the peaks in the 1100–1350 cm^{-1} window obtained on the basis of the QM/MM calculation is listed in Table 1 together with the previous findings of Egawa et al. [17].

In order to prove that the observed difference bands are indeed caused by a protonation of the propionic acid and not by protonation of a nearby water molecule, additional Raman H/D difference calculations were performed for the latter scenario. Here no difference bands were observable in the relevant wave number range (see Fig. S2). Thus, we exclude that a protonated water molecule is the origin for the observed H/D difference spectra.

4. Discussion

One of the most prominent negative bands in trace A and C of Fig. 3 occurs at 1179 cm^{-1}, which we assign to the protonated PrD*a*, in contrast to Egawa's work, which related this band to a CH_2-deformation mode at heme a_3. The present calculations assign the latter mode to a peak detected at 1149 cm^{-1}. A similar contradictory assignment occurs for the band at 1215 cm^{-1}, detected in the SERR-spectra at slightly higher wave numbers. The strongest negative band at 1250 cm^{-1} could not be assigned to a single protonation state and might represent either a protonated PrDa_3, PrAa_3, PrA*a* or a combination of all three. Interestingly, this unambiguous assignment of the band at 1250 cm^{-1} does not contradict the experiments, since in the fully reduced enzyme we can conclude from the occurrence of other bands that at least three of the four propionates (PrDa_3, PrD*a* and PrA*a*) are transiently protonated. The forth propionate PrAa_3 might be protonated as well, however we do not have any additional information about it, since protonation of PrAa_3 does not show any significant H/D sensitivity. However, if charge neutrality prevails only one propionate per heme should be protonated under equilibrium conditions. Therefore, we conclude that the protons most likely hop between the different acidic groups, which would be feasible as for both hemes the crystal structure shows a water molecule placed between the A and D propionates, respectively (See Fig. 1). Such a picture is in agreement with recent calculations that show exchange of protons between all four propionic acids [35]. Furthermore our data show that H/D exchange is possible at PrA*a* and

Table 1
Experimental observed vibrational frequencies in the resonance Raman spectra of C*c*O and their corresponding assignment to the respective protonated propionic acid stated by Ref. [17] and this work.

Ref. [17]		This work	
Frequency of H_2O—D_2O difference band [cm^{-1}]	Protonated heme propionic acid	Frequency of H_2O—D_2O difference band [cm^{-1}]	Protonated heme propionic acid
		1149	PrDa_3
1179	PrAa_3	1179	PrD*a*
1215	PrA*a*	1218	PrDa_3
1232	PrDa_3	1232	PrDa_3
1250	PrD*a*	1250	PrDa_3, PrAa_3, (PrA*a*)
		1283	PrA*a*
1306	PrX*a*	1304	PrDa_3, PrAa_3
		1330	PrA*a*

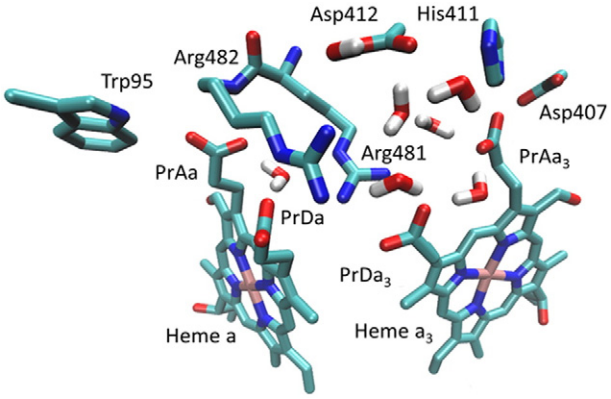

Fig. 1. Structure of the heme a and a_3 environment of C*c*O from *Rhodobacter sphaeroides* (PDB 1M56).

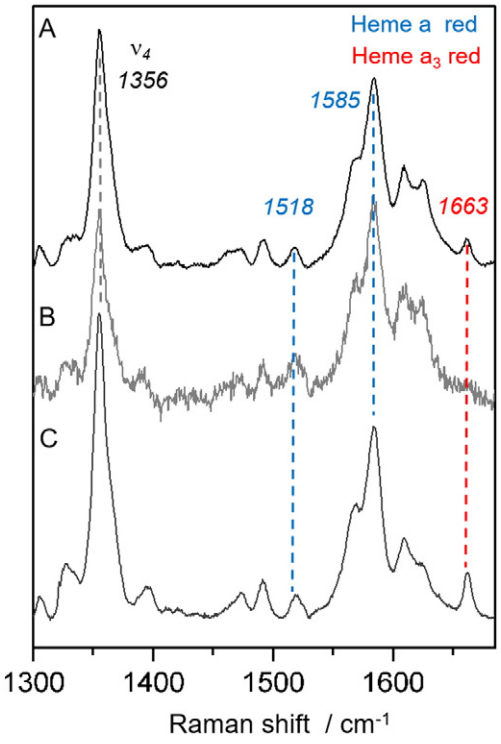

Fig. 2. SERR spectra of C*c*O in the high frequency region recorded under different conditions. (A) Open circuit potential, traces of oxygen and presence of dithionite, (B) electrode potential of −250 mV and traces of oxygen, (C) electrode potential of −400 mV in the absence of oxygen. The peaks assigned with blue numbers are associated with reduced heme *a*, whereas the peak assigned with a red number is associated with reduced heme a_3. All potentials are presented vs. Ag/AgCl. Laser excitation is 442 nm.

PrD*a* and therefore these propionates are accessible for external protons. These findings are in agreement with the measurements of Behr et al. [13], who observed a protonated PrD*a* in the fully reduced enzyme using C*c*O variants with ^{13}C modified propionic acids. However, in their work, PRD*a* was considered to be the only protonated propionic acid, whereas we observe partial protonation of at least three propionates when both hemes are reduced. From electrostatic considerations, heme *a* reduction would favor protonation of one of its own propionates [36,37]. However, as this process would terminate further electron and proton movement, direct proton transfer from Glu286 to PrD*a* must be highly inefficient. Only in a situation, where heme a_3 is reduced, protonation of PrD*a* would not hinder further progression of the oxygen reaction and the proton pumping process. This is in line with our results: we do not see a protonated PrD*a* if heme a_3 is oxidized ruling out a sufficiently fast protonation of PrD*a*.

Electrochemical reduction of C*c*O in presence of low oxygen concentration leads to the observation of reduced heme *a* and oxidized heme a_3. The concomitant H/D measurements show that the band at 1179 cm^{-1} is no more visible. Thus, under turnover conditions PrD*a* is not protonated although heme *a* is observed in its reduced state. The only still visible band at 1250 cm^{-1} has been assigned before to either a protonated PrA*a* or a protonated heme a_3 propionate. Traces of negative bands at 1218 cm^{-1} and 1304 cm^{-1} (now shifted to 1216 cm^{-1} and 1310 cm^{-1}) might be present in trace B of Fig. 3 while the band at 1283 cm^{-1} has definitely disappeared. This observation points to a protonation of one of the heme a_3 propionates rather than PrA*a* but the spectra are too noisy to draw final conclusions from them alone. It is important to note that the intensity of the band at 1250 cm^{-1} is always increased if oxygen is present (trace A and B in Fig. 3) compared to conditions with no oxygen (trace C in Fig. 3). The presence of oxygen should not affect PrA*a*, but will of course have an impact on the propionates of heme a_3. Hence, combining these observations for oxygen conditions we confidently assign the 1250 cm^{-1} band to a protonated heme a_3 propionic acid. However, an alternative assignment to PrA*a*, although very unlikely, cannot be ruled out completely. The proposed redox and protonation states of heme *a* and heme a_3 under the three conditions discussed in this study are summarized schematically in Fig. 5. Experimental determination of the Cu_B oxidation state was not possible with the present setup. Accordingly, we cannot state explicitly whether a chemical proton might have been transferred to the BNC under our measured steady state conditions or not. In the computations the Cu_B(I) state was assumed.

To distinguish between a protonated PrDa_3 or PrAa_3 is difficult and alone from our data no final conclusion can be drawn. However, as we have pointed out before that PrAa_3 shows much less sensitivity to H/D exchange than PrDa_3. This would favor the interpretation of a protonated PrDa_3 in trace B of Fig. 3. But, the situation might change under turnover conditions and the negative band that we observe in Fig. 3 concomitant to an oxidized heme a_3 is really small. In contrast to PrDa_3, PrAa_3 does not form a salt bridge. In the crystal structure of *R. sphaeroides*, (PDB 2GSM) [38], the distance between a PrAa_3 oxygen and an Asp407 oxygen is only 2.45 Å. Such a short distance is only possible if the acidic groups of PrAa_3 and Asp407 share a proton. Thus, it is possible that PrAa_3 is partially protonated all the time, which could explain that we cannot make a clear conclusion on the protonation state of PrAa_3. Nevertheless, comparative H/D SERRS measurements at +90 mV under anaerobic conditions and at open circuit potential with oxygen present - both corresponding to conditions where we observe hemes *a* and a_3 more or less in their oxidized state - do not show the presence of a band at 1250 cm^{-1} (Fig. S2). This clearly indicates that detection of this band is associated with significant heme *a* reduction.

In summary we do see protonation of at least one of the heme a_3 propionates concomitant to a reduced heme *a* and an oxidized heme a_3. A reasonable interpretation of this finding is only possible if heme a reduction leads at least to transient protonation of PrDa_3 prior to heme a_3 reduction, which would support its role as a PLS in the proton pumping process. Whether we actually observe in the vibrational spectra a protonated PrDa_3 or PrAa_3 does not alter this interpretation, since in both cases the data support proton transportation via the heme a_3 propionates. Since PrAa_3 is most likely not the direct proton acceptor from Glu286 and we could show that in the fully reduced enzyme PrDa_3 is protonated for some time, a proton pathway via PrDa_3-PrAa_3 seems to be highly probable.

The question remains whether PrD*a* participates also in the proton translocation pathway. A protonated PrD*a* is observed in combination with a reduced heme a_3 in case that oxygen and chemical reductants are present (Fig. 3 trace A) and oxygen binding is the rate limiting step. The presence of a protonated PrD*a* under these conditions

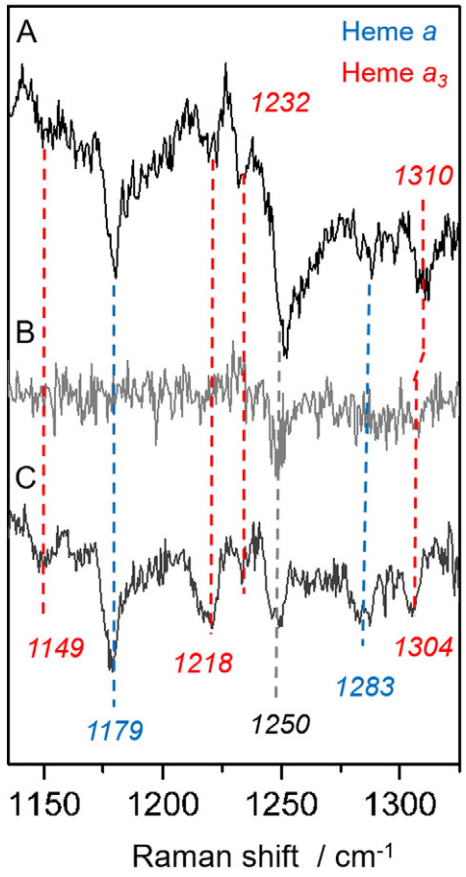

Fig. 3. H_2O minus D_2O SERR difference spectra of CcO attached to electrodes recorded under different conditions. (A) Open circuit potential, traces of oxygen and presence of dithionite, (B) electrode potential of −250 mV and traces of oxygen, (C) electrode potential of −400 mV in the absence of oxygen. All potentials are presented vs. Ag/AgCl. Laser excitation is 442 nm.

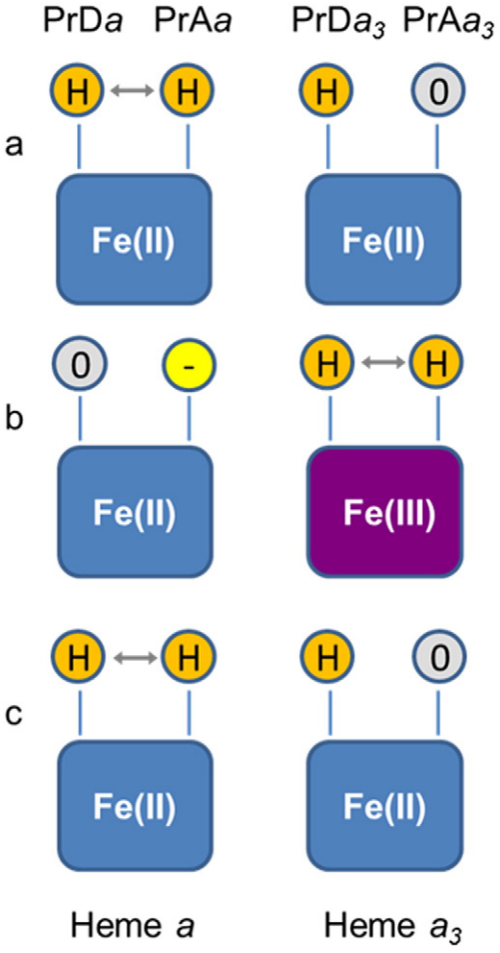

Fig. 5. Schematic representation of the proposed redox states of the hemes and the protonation state of the respective propionic acids under different conditions. (a) Open circuit potential, traces of oxygen and presence of dithionite, (b) electrode potential of −250 mV and traces of oxygen, (c) electrode potential of −400 mV in the absence of oxygen. The propionates are protonated (H), deprotonated (−) or the protonation state could not be determined (0). The arrows indicate possible proton transfer between two propionate chains, such that only one propionate at a time will be protonated.

indicates that its protonation has to occur at least on the same timescale as oxygen binding. This observation could be explained if protonation of PrDa_3 initiates conformational changes of the nearby arginines that make proton transfer to PrD*a* more effective. Our findings indicate that PrD*a* might be more actively involved in the proton pumping process than so far assumed. It could function as an additional proton storage site under conditions where oxygen supply is low. Such a scenario would stabilize the interplay between electron transfer and proton translocation under varying oxygen concentrations.

5. Conclusions

SERR spectroscopy in combination with QM/MM calculations was applied to identify the protonation states of the heme *a* and heme a_3

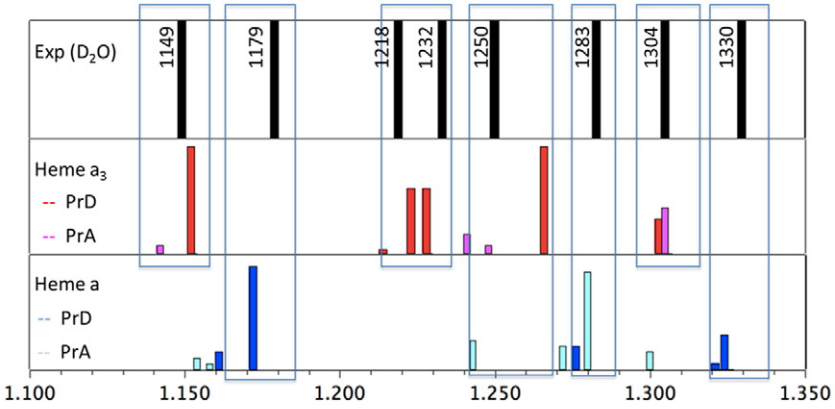

Fig. 4. Experimental vibrational frequencies of CcO in D_2O buffer in the 1100–1350 cm^{-1} window (top) and calculated QM/MM vibrational frequencies of deuterated heme a_3 (middle) and heme *a* (bottom). Only those normal modes which are Raman active and have significant contributions of PrA and PrD side chains are considered. The heights in the bar-plots quantitatively represent the probability of detecting a vibrational mode in a H_2O—D_2O SERRs difference experiment, which is given by the change in frequency or Raman intensity upon H/D exchange.

propionates as a function of the individual heme redox states. The chemically reduced C*c*O in presence of low concentration of oxygen and the electrochemical reduced C*c*O in absence of oxygen showed both the presence of reduced heme *a* and heme a_3 as well as protonation of the propionates PrD*a*, PrA*a* and PrDa_3, corresponding to heme *a* and heme a_3, respectively. The protonation state of PrAa_3 was experimentally not accessible. The explanation for it could be that PrAa_3 and Asp407 share a proton under all considered experimental conditions. Electrochemically reduced C*c*O in presence of low concentration of oxygen reveals under steady state condition a reduced heme *a* and an oxidized heme a_3. In this situation, only one vibrational Raman band could be observed that we assign to one of the heme a_3 propionic acids. This observation can be considered as direct evidence that heme *a* reduction leads at least transiently to protonation of one of the two propionates of heme *a* prior to heme a_3 reduction. The interpretation of our experimental data supports a reaction mechanism in C*c*O where PrDa_3 and PrAa_3 act as transient proton loading sites.

Transparency document

The transparency document associated with this article can be found, in online version.

Acknowledgements

We would like to thank Claudia Schulz and Dorothea Heinrich for the preparation of C*c*O and Joachim Heberle and Peter Hildebrandt for helpful discussions. Financial support by the DFG (CRC 1078 A1, B4, C2, C3) is gratefully acknowledged.

Appendix A. Supplementary data

Supplementary data to this article can be found online at http://dx.doi.org/10.1016/j.bbabio.2016.10.009.

References

[1] P. Brzezinski, R.B. Gennis, Cytochrome c oxidase: exciting progress and remaining mysteries, J. Bioenerg. Biomembr. 40 (2008) 521–531.
[2] D.A. Proshlyakov, M.A. Pressler, G.T. Babcock, Dioxygen activation and bond cleavage by mixed-valence cytochrome c oxidase, Proc. Natl. Acad. Sci. U. S. A. 95 (1998) 8020–8025.
[3] T. Ogura, S. Hirota, D.A. Proshlyakov, K. Shinzawaltoh, S. Yoshikawa, T. Kitagawa, Time-resolved resonance Raman elucidation of the pathway for dioxygen reduction by cytochrome c oxidase, J. Am. Chem. Soc. 115 (1993) 8527–8536.
[4] S. Han, Y.C. Ching, D.L. Rousseau, Ferryl and hydroxy intermediates in the reaction of oxygen with reduced cytochrome c oxidase, Nature 348 (1990) 89–90.
[5] M. Wikström, V. Sharma, V.R.I. Kaila, J.P. Hosler, G. Hummer, New perspectives on proton pumping in cellular respiration, Chem. Rev. 115 (2015) 2196–2221.
[6] A.V. Pisliakov, P.K. Sharma, Z.T. Chu, M. Haranczyk, A. Warshel, Electrostatic basis for the unidirectionality of the primary proton transfer in cytochrome c oxidase, Proc. Natl. Acad. Sci. U. S. A. 105 (2008) 7726–7731.
[7] P. Goyal, S. Yang, Q. Cui, Microscopic basis for kinetic gating in cytochrome c oxidase: insights from QM/MM analysis, Chem. Sci. 6 (2015) 826–841.
[8] V.R.I. Kaila, V. Sharma, M. Wikström, The identity of the transient proton loading site of the proton-pumping mechanism of cytochrome c oxidase, Biochim. Biophys. Acta 1807 (2011) 80–84.
[9] S. Chakrabarty, I. Namslauer, P. Brzezinski, A. Warshel, Exploration of the cytochrome c oxidase pathway puzzle and examination of the origin of elusive mutational effects, Biochim. Biophys. Acta 1807 (2011) 413–426.
[10] D.M. Popović, A.A. Stuchebrukhov, Coupled electron and proton transfer reactions during the O → E transition in bovine cytochrome c oxidase, Biochim. Biophys. Acta Bioenerg. 1817 (2012) 506–517.
[11] A.-L. Johansson, S. Chakrabarty, C.L. Berthold, M. Högbom, A. Warshel, P. Brzezinski, Proton-transport mechanisms in cytochrome c oxidase revealed by studies of kinetic isotope effects, Biochim. Biophys. Acta 1807 (2011) 1083–1094.
[12] J. Behr, P. Hellwig, W. Mäntele, H. Michel, Redox dependent changes at the heme propionates in cytochrome c oxidase from *Paracoccus denitrificans*: direct evidence from FTIR difference spectroscopy in combination with heme propionate ^{13}C labeling, Biochemistry 37 (1998) 7400–7406.
[13] J. Behr, H. Michel, W. Mäntele, P. Hellwig, Functional properties of the heme propionates in cytochrome c oxidase from *Paracoccus denitrificans* evidence from FTIR difference spectroscopy and site-directed mutagenesis, Biochemistry 39 (2000) 1356–1363.
[14] M. Sakaguchi, K. Shinzawa-Itoh, S. Yoshikawa, T. Ogura, A resonance Raman band assignable to the O-O stretching mode in the resting oxidized state of bovine heart cytochrome c oxidase, J. Bioenerg. Biomembr. 42 (2010) 241–243.
[15] C. Varotsis, Y. Zhang, E.H. Appelman, G.T. Babcock, Resolution of the reaction sequence during the reduction of O_2 by cytochrome-oxidase, Proc. Natl. Acad. Sci. U. S. A. 90 (1993) 237–241.
[16] J. Kozuch, I. von der Hocht, F. Hilbers, H. Michel, I.M. Weidinger, Resonance Raman characterization of the ammonia-generated oxo intermediate of cytochrome c oxidase from *Paracoccus denitrificans*, Biochemistry 52 (2013) 6197–6202.
[17] T. Egawa, H.J. Lee, H. Ji, R.B. Gennis, S.R. Yeh, D.L. Rousseau, Identification of heme propionate vibrational modes in the resonance Raman spectra of cytochrome c oxidase, Anal. Biochem. 394 (2009) 141–143.
[18] T. Egawa, S.R. Yeh, D.L. Rousseau, Redox-controlled proton gating in bovine cytochrome c oxidase, PLoS One 8 (2013).
[19] M. Sezer, P. Kielb, U. Kuhlmann, H. Mohrmann, C. Schulz, D. Heinrich, R. Schlesinger, J. Heberle, I.M. Weidinger, Surface enhanced resonance Raman spectroscopy reveals potential induced redox and conformational changes of cytochrome c oxidase on electrodes, J. Phys. Chem. B 119 (2015) 9586–9591.
[20] J. Hrabakova, K. Ataka, J. Heberle, P. Hildebrandt, D.H. Murgida, Long distance electron transfer in cytochrome c oxidase immobilised on electrodes. A surface enhanced resonance Raman spectroscopic study, Phys. Chem. Chem. Phys. 8 (2006) 759–766.
[21] M. Sezer, R. Spricigo, T. Utesch, D. Millo, S. Leimkuehler, M.A. Mroginski, U. Wollenberger, P. Hildebrandt, I.M. Weidinger, Redox properties and catalytic activity of surface-bound human sulfite oxidase studied by a combined surface enhanced resonance Raman spectroscopic and electrochemical approach, Phys. Chem. Chem. Phys. 12 (2010) 7894–7903.
[22] P. Kielb, M. Sezer, S. Katz, F. Lopez, C. Schulz, L. Gorton, R. Ludwig, U. Wollenberger, I. Zebger, I.M. Weidinger, Spectroscopic observation of calcium-induced reorientation of cellobiose dehydrogenase immobilized on electrodes and its effect on electrocatalytic activity, ChemPhysChem 16 (2015) 1960–1968.
[23] H.K. Ly, M. Sezer, N. Wisitruangsakul, J.J. Feng, A. Kranich, D. Millo, I.M. Weidinger, I. Zebger, D.H. Murgida, P. Hildebrandt, Surface-enhanced vibrational spectroscopy for probing transient interactions of proteins with biomimetic interfaces: electric field effects on structure, dynamics and function of cytochrome c, Febs J. 278 (2011) 1382–1390.
[24] S. Todorovic, M.M. Pereira, T.M. Bandeiras, M. Teixeira, P. Hildebrandt, D.H. Murgida, Midpoint potentials of hemes a and a3 in the quinol oxidase from *Acidianus ambivalens* are inverted, J. Am. Chem. Soc. 127 (2005) 13561–13566.
[25] G. Cohen-Bazire, W.R. Sistrom, R.Y. Stanier, Kinetic studies of pigment synthesis by non-sulfur purple bacteria, J. Cell. Physiol. 49 (1957) 25–68.
[26] D.M. Mitchell, R.B. Gennis, Rapid purification of wild-type and mutant cytochrome c oxidase from *Rhodobacter sphaeroides* by Ni^{2+}-affinity chromatography, FEBS Lett. 368 (1995) 148–150.
[27] H. Wackerbarth, U. Klar, W. Gunther, P. Hildebrandt, Novel time-resolved surface-enhanced (resonance) Raman spectroscopic technique for studying the dynamics of interfacial processes: application to the electron transfer reaction of cytochrome c at a silver electrode, Appl. Spectrosc. 53 (1999) 283–291.
[28] A.D. MacKerell, D. Bashford, R.L. Dunbrack, J.D. Evanseck, M.J. Field, S. Fischer, J. Gao, H. Guo, S. Ha, D. Joseph-McCarthy, et al., All-atom empirical potential for molecular modeling and dynamics studies of proteins, J. Phys. Chem. B 102 (1998) 3586–3616.
[29] D. Bakowies, W. Thiel, Hybrid models for combined quantum mechanical and molecular mechanical approaches, J. Phys. Chem. 100 (1996) 10580–10594.
[30] P. Sherwood, A.H. de Vries, M.F. Guest, G. Schreckenbach, C.R.A. Catlow, S.A. French, A.A. Sokol, S.T. Bromley, W. Thiel, A.J. Turner, S. Billeter, F. Terstegen, S. Thiel, J. Kendrick, S.C. Rogers, J. Casci, M. Watson, F. King, E. Karlsen, M. Sjøvoll, et al., QUASI: a general purpose implementation of the QM/MM approach and its application to problems in catalysis, J. Mol. Struct. THEOCHEM 632 (2003) 1–28.
[31] M.A. Mroginski, F. Mark, W. Thiel, P. Hildebrandt, Quantum mechanics/molecular mechanics calculation of the Raman spectra of the phycocyanobilin chromophore in alpha-C-phycocyanin, Biophys. J. 93 (2007) 1885–1894.
[32] D.H. Murgida, P. Hildebrandt, Active-site structure and dynamics of cytochrome c immobilized on self-assembled monolayers - a time-resolved surface enhanced resonance Raman spectroscopic study, Angew. Chem. Int. Ed. 40 (2001) 728–731.
[33] G.E. Heibel, P. Hildebrandt, B. Ludwig, P. Steinrucke, T. Soulimane, G. Buse, Comparative resonance Raman-study of cytochrome-c-oxidase from beef-heart and *Paracoccus denitrificans*, Biochemistry 32 (1993) 10866–10877.
[34] M.G. Friedrich, F. Giebeta, R. Naumann, W. Knoll, K. Ataka, J. Heberle, J. Hrabakova, D.H. Murgida, P. Hildebrandt, Active site structure and redox processes of cytochrome c oxidase immobilised in a novel biomimetic lipid membrane on an electrode, Chem. Commun. (Camb.) (2004) 2376–2377.
[35] J. Lu, M.R. Gunner, Characterizing the proton loading site in cytochrome c oxidase, Proc. Natl. Acad. Sci. U. S. A. 111 (2014) 12414–12419.
[36] G.M. Ullmann, The coupling of protonation and reduction in proteins with multiple redox centers: theory, computational method, and application to cytochrome c3, J. Phys. Chem. B 104 (2000) 6293–6301.
[37] P. Voigt, E.W. Knapp, Tuning heme redox potentials in the cytochrome C subunit of photosynthetic reaction centers, J. Biol. Chem. 278 (2003) 51993–52001.
[38] L. Qin, C. Hiser, A. Mulichak, R.M. Garavito, S. Ferguson-Miller, Identification of conserved lipid/detergent-binding sites in a high-resolution structure of the membrane protein cytochrome c oxidase, Proc. Natl. Acad. Sci. U. S. A. 103 (2006) 16117–16122.